RSC Advances

ROYAL SOCIETY OF CHEMISTRY

www.rsc.org/advances

RSC Advances

ARTICLE

Preparation and characterization of fully renewable polybenzoxazines from monomers containing multi-oxazine rings

Received 00th January 20xx,
Accepted 00th January 20xx

DOI: 10.1039/x0xx00000x

www.rsc.org/

Lei Zhang,[a] Yejun Zhu,[a] Dan Li,[b] Min Wang,[b] Haibin Chen[a,b] and Jingshen Wu[a,b,]*

Two fully renewable benzoxazine monomers containing multi-oxazine rings were synthesized and used to prepare polybenzoxazines. The structures of the monomers, prepared from renewable feedstock (vanillin, guaiacol, octadecylamine and furfurylamine) were supported by FT-IR and NMR spectral analysis. The melting points and curing temperatures were characterized through DSC. Thermal initiated ring-opening polymerization of the monomers was monitored by FT-IR. Solubility of the polybenzoxazines were examined and cross-linking differences between polymers prepared from monomers with mono-oxazine and multi-oxazine rings were clarified. Through energy calculation, substitution was found prefered to take place at furan ring. The thermal properties were investigated through TGA, which showed good thermal stability ($T_d^{5\%}$ at 284°C and 335°C) and high char yield (up to 59.6%). The mechanical properties were characterized through DMA, which revealed a glass transition temperature at 155°C. Due to structure speciality, the polybenzoxazines also showed pH responsiveness and can reversibly change color under different conditions.

Introduction

Polybenzoxazines are a new generation of phenolic type thermosets, which inherit the excellent thermal properties of traditional phenolic resins and overcome their disadvantages, such as harsh synthesis condition and releasing volatile molecules during curing. Polybenzoxazines also possess other striking features, including structure design flexibility, low melting viscosity, near-zero curing shrinkage, low water absorption and high chemical resistance.[1] Therefore, they became some of the rare new polymers which were commercialized over the past 30 years.[2]

Due to environmental and sustainable economic concern, growing attempts have evolved from incorporating petroleum-based raw materials to natural renewable feedstock in synthesis of benzoxazine resin in the last few years.[3,4] Polybenzoxazines cannot be an exception. In fact, not only academics, but also industries have engaged in exploring renewable polybenzoxazines, since trials on developing other renewable polymers were succeeded and available in market[4].

Generally, the corresponding monomers of poly-benzoxazines, 1,3-benzoxazines, are prepared from phenols, amines and formaldehyde through Mannich condensation.[5] Till now, efforts were mainly contributed to exploring renewable phenols because renewable amines are relatively rare in both species and amounts.[4] Only a few papers based on renewable multi-amine, chitosan, have been reported.[6,7] After the first trial on 1999,[8] there was an 8 years' silence until researchers used cardanols, which can be easily isolated from cashew nut shell oil, for preparing benzoxazine monomer in 2007.[9] With the long flexible alkyl chain, the fabricated monomers can be used as reactive diluents for epoxy to enhance the toughness.[10] Urushiol based benzoxazine monomers achieves similar functions.[11] Moreover, it has lower curing temperature owing to the extra hydroxyl group on benzene ring. Eugenol, a renewable mono-phenol which can be extracted from clove, was selected to synthesize benzoxazines.[12] The additional allyl moiety was considered to enhance the cross-linking density by participating the ring-opening polymerization,[12,13] although opposite results had been reported as well.[14] Besides phenols extracted from specific plants, increasing researchers have focused on lignin-derived phenols recently due to the unique ultra-abundant stock in nature.[15] In 2012, two fully renewable bio-based benzoxazine monomers were prepared from guaiacol, which is a lignin derivative.[16] The thermal stability was enhanced by copolymerization of the two monomers. In 2013, "lignin-like" coumaric acid, ferulic acid and phloretic acid as well as the corresponding esters were used to prepare benzoxazine monomers.[1] Electron withdrawing effect of the carboxyl group was found to deteriorate the thermal stability of the monomers when unsaturated chain conjugates with benzene ring. Vanillin, which is another renewable phenol, has been widely used in food industry as a flavour. It can now be industrially manufactured from lignin within the waste of paper industry.[17] In 2014, vanillin based benzoxazine

a. Department of Mechanical and Aerospace Engineering, The Hong Kong University of Science and Technology, Clear Water Bay, Kowloon, Hong Kong. E-mail: mejswu@ust.hk
b. Center for Engineering Materials and Reliability, Fok Ying Tung Research Institute, The Hong Kong University of Science and Technology, Nansha, China.
† Footnotes relating to the title and/or authors should appear here.
Electronic Supplementary Information (ESI) available: [details of any supplementary information available should be included here]. See DOI: 10.1039/x0xx00000x

monomers were reported simultaneously by H. Ishida and I. K. Varma.[18,19] The aldehyde group can help decrease the curing temperature as well as be further functionalized into a reactive surfactant. But it will also generate CO_2 during polymerization, which may limit its application for preparing bulk materials.[19]

Although several renewable benzoxazine monomers had been prepared so far, most of them have only one oxazine ring in the monomer. However, rather than polymers with high molecular weight, these monomers generate merely oligomers of four to six repeating units.[20] The ring-opening polymerization was obstructed by the intramolecular hydrogen bonding.[21,22] As a consequence, the products prepared from monomers with one oxazine ring may not suitable for structure applications.[23] Fortunately, monomers or pre-polymers with multi-oxazine rings can overcome the trouble,[24,25] but the corresponding precursors have to contain multi-phenol, multi-amine or aminophenol structures.[26,27] However, the monomers prepared from multi-phenols so far, such as terpenediphenol and 4,4-bis (hydroxyphenyl) pentanoic acid, and more recently, cardbisphenol, are just partially renewable.[8,28,29] Meanwhile, due to rare amine variety in nature, past benzoxazine monomers with multi-oxazine rings were synthesized from renewable mono-phenol, but petroleum-derived multi-amines.[30] In regard to aminophenols, only one paper published till now due to the species restriction.[27] On the other hand, monomers with functional groups can react with other moieties to achieve multi-oxazine structures. However, it requires other renewable precursors containing specific reactive groups, which complicates the process and restricts feedstock selection.[31] As a result, the challenge remains.

This study focuses on the synthesis and characterization of two polybenzoxazines cured from fully renewable monomers with multi-oxazine rings. First, a fully renewable triphenol was prepared from vanillin and guaiacol. Then, it reacted with octadecylamine and furfurylamine, which are derived from furfural and vegetable oil, to produce the benzoxazines. The monomers' structures, polymerization process, thermal and mechanical properties were supported by Fourier transform infrared spectroscopy (FT-IR), nuclear magnetic resonance spectroscopy (NMR), mass spectroscopy (MS), differential scanning calorimetry (DSC), thermogravimetric analysis (TGA) and dynamic mechanical analysis (DMA), respectively. Due to the particular chemical structures, the polymers exhibited reversible color changes under different pH conditions.

Experimental

Materials

All reagents used for synthesis are commercially available. Vanillin (99%), guaiacol (99%) and $CDCl_3$ (with 0.03 vol. % of TMS as reference) were purchased from Aladdin Reagent (Shanghai) Co., Ltd., China. Furfurylamine (99%) was obtained from J&K Scientific. Paraformaldehyde (96%), sodium sulfate anhydrous (99%), potassium bromide (99.5%) and octadecylamine (90%) were acquired from Sigma-Aldrich. Sodium hydroxide (99%), chloroform (99%) and sulfuric acid (95%) were purchased from VWR. Absolute ethanol (99.9%) was obtained from Merck. All the above chemicals were used as received.

Measurements

The FT-IR spectra of the compounds' structures and the curing process were recorded by a Bruker FT-IR spectrometer. KBr pellet technique was used with 16 scans at a 4 cm^{-1} resolution. The structures of the compounds were verified by nuclear magnetic resonance spectroscopy (^{1}H-NMR and ^{13}C-NMR) using a Varian Mercury VX 300 NMR. The characterization procedure was conducted under room temperature with deuterated chloroform ($CDCl_3$) as solvent and tetramethylsilane (TMS) as internal standard. The molecular weight was detected by a MALDI Micro MX mass spectroscopy by Waters MICROMASS.

The thermal stability and char yield of the monomers and cured polymers were studied with a TA Instrument Q50 TGA which equipped with a nitrogen flow rate of 25 ml/min. The heating rate was 10K/min if not specifically illustrated. The masses of all samples were about 5 mg. The polymerization process and the glass transition temperatures (T_g) were monitored by a DSC from TA Instrument, Q2000. The scan rates were set at 10K/min under nitrogen atmosphere. The T_g was obtained through two heating scans of the cured samples. The middle point between the tangent lines of the steps was defined as T_g. All samples with mass of 1-3 mg were sealed in lids covered aluminum pans. DMA was performed using a TA Instrument, Q800, at a heating rate of 5K/min from room temperature to 30°C above T_g. The samples were tested under three-point bending mode with a frequency of 1Hz and displacement of 10 μm after moulded into 70 mm x 10 mm x [illegible] mm bars. The solubility of the cured polymers were determined by the weight change before and after Soxhlet extraction for 24 hours using chloroform as solvent. The residues after extraction were dried under vacuum oven for 12 hours under 60°C before weighing.

Methods

Synthesis of 4,4',4"-trihydroxy-3,3',3"-trimethyoxy-triphenyl-methane [TP]. Vanillin (7.5 g, 50 mmol) and guaiacol (12.4 g, 100 mmol) were dissolved using 8 mL anhydrous ethanol in a 250 mL flask. 8 mL of sulfuric acid was mixed with 8 mL of anhydrous ethanol and kept in a charging hopper. The flask was maintained at a temperature below 5°C before gradually introducing the acidic ethanol solution. The mixture was gently stirred under N_2 atmosphere and a temperature below 10°C for more than 12 hours to generate a dark red turbid solution. The mixture was then washed by distilled water until it became neutral. The solid was crystallized through chloroform and filtered, to obtain the pale pink needle-like crystals of [4,4',4"-trihydroxy-3,3',3"-trimethyoxy-triphenyl-methane] [TP]. Yield: 67%, m.p. 125°C-128°C. MALDI mass: m/z=381.2 (positive mode), 380 (negative mode).

FT-IR (KBr, cm^{-1}) 3400 (O-H), 3053 (C-H, Ar), 2940 and 2850 (C-H), 1614 (C=C, Ar), 1508 (C-H, Ar), 1269 and 1033 (C-O-C), 870 and 756 (Ar); ^{1}H-NMR ($CDCl_3$, ppm) 6.81 (Ar-H, 3H), 6.62 (Ar-H, 3H), 6.57 (Ar-H, 3H), 5.50 (Ph-OH), 5.34 ($(Ar)_3$-CH, 1H), 3.78 (O-CH_3, 9H); ^{13}C-NMR ($CDCl_3$, ppm) 146.29, 143.91, 136.41, 121.98, 113.93, 111.87, 55.86 (O-CH_3), 55.66 (Ar_3-CH).

Synthesis of Tris(8-methoxy-3-octadecyl-3,4-dihydro-2H-1,3-benzoxazin-6-yl)methane [Bz_TPo]. In a 250 mL flask, TP (10 mmol), paraformaldehyde (2.0 g, excess) and n-octadecylamine (30 mmol) was added with 80 mL of chloroform. 20 mL of anhydrous ethanol was introduced to benefit the solubility of TP. The solution was refluxed for 20 hours resulted in an orange transparent solution. The solution was washed by 1 N sodium hydroxide solution for several times and followed by distilled water until the solution became neutral. The solution was dried with anhydrous sodium sulfate and filtered to obtain a transparent solution. The solvent was evaporated before further purified in anhydrous ethanol to acquire a white powder. Yield: 72%, m.p. 50°C. MALDI mass: m/z=1263.0 (positive mode).

FT-IR (KBr, cm^{-1}): 2920 and 2850 (C-H), 1589 (C=C, Ar), 1497 (C-H, Ar), 1320 (CH_2 wagging), 1226 and 1097 (C-O-C), 1147 (C-N-C), 925 (oxazine ring), 856 and 719 (Ar); ^{1}H-NMR ($CDCl_3$, ppm): 6.49 (Ar-H, 3H), 6.24 (Ar-H, 3H), 5.21 ($(Ar)_3$-CH, 1H), 4.93 (N-CH_2-O, 6H), 3.91 (N-CH_2-Ar, 6H), 3.76 (O-CH_3, 9H), 2.74, 1.25, 0.88 (N-$C_{18}H_{37}$); ^{13}C-NMR ($CDCl_3$, ppm): 147.35, 141.88, 135.79, 120.31, 119.91, 110.64, 82.76, 55.80, 55.78, 51.57, 50.29, 15-35.

Synthesis of Tris(8-methoxy-3-furfuryl-3,4-dihydro-2H-1,3-benzoxazin-6-yl) methane [Bz_TPf]. The synthesis process of Bz_TPf monomer was similar as synthesis of Bz_TPo except for adding furfurylamine (30 mmol) instead of n-octadecylamine. White powder was obtained after further purified in ethanol. Yield: 65%, m.p. 165°C. MALDI mass: m/z=746.4 (positive mode).

FT-IR (KBr, cm^{-1}):3141 and 3114 (C-H, furan ring), 3062 (C-H, Ar), 2931, 2904 and 2830 (C-H), 1591 (C=C, Ar), 1495 (C-H, Ar), 1321 (CH_2, wagging), 1222 and 1094 (C-O-C), 1148 (C-N-C), 920 (oxazine ring), 850 and 735 (Ar).

^{1}H-NMR ($CDCl_3$, ppm): 7.40 (C=CH-O, 3H), 6.53 (Ar-H, 3H), 6.32 (C=CH-C, 3H), 6.25 (Ar-H, 3H), 6.24 (C=CH-C, 3H), 5.22 ($(Ar)_3$-CH, 1H), 4.96 (N-CH_2-O, 6H), 3.96 (N-CH_2-Ar, 6H) 3.95(N-CH_2-C, 6H), 3.80 (O-CH_3, 9H); ^{13}C-NMR ($CDCl_3$, ppm): 151.53, 147.47, 142.57, 141.66, 136.05, 119.88, 119.67, 110.83, 110.18, 108.89, 82.25, 55.87, 55.85, 49.43, 48.38.

Synthesis of 8-methoxy-3-octadecyl-3,4-dihydro-2H-1,3-benzoxazine [Bz_Go]. For comparison, two other monomers with mono-oxazine ring were synthesized. In order to avoid differences caused by preparation method, solvent method was used instead of solventless method reported by X. D. Liu et al.[16] Specifically, guaiacol (12.4 g, 100mmol), paraformaldehyde (6.6 g, excess) and n-octadecylamine (100 mmol) was dissolved and added into a 250 mL flask. After refluxing for over 20 hours, a pale yellow solvent was obtained. By successively washing with 1 N sodium hydroxide solution and distilled water for several times until the solution became neutral. The solvent was then evaporated to leave a pale yellow powder. It was purified by ethanol to obtain a white powder. Yield: 75%, m.p. 60-62°C. MALDI mass: m/z=418.4 (positive mode).

FT-IR (KBr, cm^{-1}): 2920 and 2851 (C-H), 1583 (C=C, Ar), 1487 (C-H, Ar), 1317 (CH_2, wagging), 1224 and 1076 (C-O-C), 1159 (C-N-C), 916 (oxazine ring), 734 (Ar). (Figure S1)

^{1}H-NMR ($CDCl_3$, ppm): 6.82 (Ar-H, 1H), 6.75 (Ar-H, 1H), 6.59 (Ar-H, 1H), 4.96 (N-CH_2-O, 2H), 4.00 (N-CH_2-Ar, 2H), 3.87 (O-CH_3, 3H), 2.74, 1.25, 0.88 (N-$C_{18}H_{37}$); ^{13}C-NMR ($CDCl_3$, ppm): 147.59, 143.54, 120.80, 119.79, 119.37, 109.28, 82.83, 55.76, 51.43, 50.01, 15-35. (Figure S2)

Synthesis of 8-methoxy-3-furfuryl-3,4-dihydro-2H-1,3-benzoxazine [Bz_Gf]. The synthesis process of Bz_Gf was similar as synthesis of Bz_Go except for adding furfurylamine (100 mmol) instead of n-octadecylamine. It was recrystallized from ethanol to obtain a white crystal. Yield: 70%, m.p. 90-92°C. MALDI mass: m/z=246.1 (positive mode).

FT-IR (KBr, cm^{-1}):3153 and 3124 (C-H, furan ring), 3093 (Ar-H), 2958, 2941, 2913 and 2836 (C-H), 1583 (C=C, Ar), 1485 (C-H, Ar), 1338 (CH_2, wagging), 1267 and 1074 (C-O-C), 1149 (C-N-C), 924 (oxazine ring), 732 (Ar). (Figure S3)

^{1}H-NMR ($CDCl_3$, ppm): 7.42 (C=CH-O, 1H), 6.85 (Ar-H, 1H), 6.78 (Ar-H, 1H), 6.60 (Ar-H, 1H), 6.33 (C=CH-C, 1H), 6.26 (C=CH-C, 1H), 5.00 (N-CH_2-O, 2H), 4.02 (N-CH_2-Ar, 2H), 3.96 (N-CH_2-C, 2H), 3.89 (O-CH_3, 3H); ^{13}C-NMR ($CDCl_3$, ppm): 151.57, 147.69, 143.25, 142.60, 120.20, 120.14, 119.44, 110.17, 109.52, 109.00, 82.41, 55.82, 49.08, 48.29. (Figure S4)

Calculation

The energy calculations were performed to study the competed substitutions on furan ring and benzene ring of Bz_TPf. The energy difference between the iminium intermediate and different transition state of substitution was evaluated. The calculations were made on a Gaussian09[32] using the density functional theory (DFT) under B3LYP functional and 6-31G+(d,p) basis sets. All of the structures were optimized before frequency calculation. The transition states were checked with unique virtual frequency. IRC analysis was applied to examine the structures as well.

Results and discussion

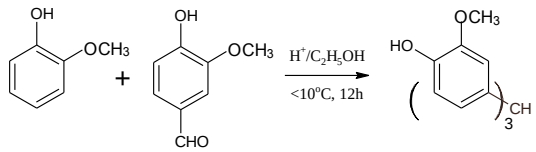

Scheme 1 Synthesis of TP.

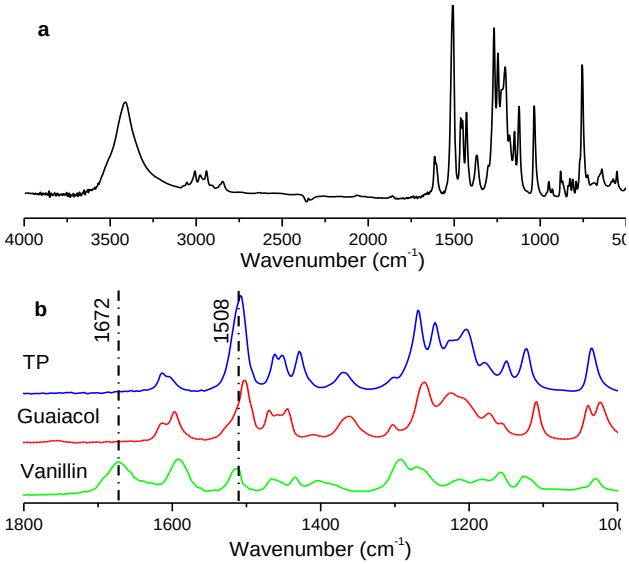

Fig. 1 FT-IR spectra of (a) TP and (b) comparison between TP, guaiacol and vanillin**.**

Synthesis of TP was carried out through a phenol-aldehyde condensation reaction under acid catalysis (Scheme 1). The chemical structures were confirmed by FT-IR and NMR spectral methods. Figure 1(a) shows the FT-IR spectrum of TP. The absorbance peak near 3400 cm^{-1} indicates the –OH group. The peaks at 3053 and 3010 cm^{-1} are the stretching of C-H on benzene ring. The peaks around 2850-2980 cm^{-1} are the C-H stretching of methyl group. As shown in Figure 1(b), the peak around 1672 cm^{-1} represents the aldehyde group of vanillin. This peak is absence in FT-IR of TP, which means the participation of the aldehyde group in the reaction. The peak at 1614 cm^{-1} is the stretching of the benzene ring. Comparing with guaiacol and vanillin, the absorbance at 1508 cm^{-1} confirms the trisubstituted benzene ring. The peaks at 1269 and 1033 cm^{-1} are attributed to the asymmetric and symmetric stretching of the C-O-C. The preparation of the benzoxazine monomers from TP was implemented through Mannich condensation with paraformaldehyde, n-octadecyl-amine and furfurylamine (Scheme 2). The high absorbance intensity at 2920 and 2850 cm^{-1} in Figure 2(a) represents the long alkyl chain of Bz_TPo. New absorbance peaks at 1320 and 925 cm^{-1} confirms the formation of the oxazine ring. This is also proved by the substitution change on benzene ring indicated by the peaks shifting from 1508 to 1497 cm^{-1}.[18] Similar results can be found in Figure 2(b), which shows the FT-IR spectrum of Bz_TPf. The absorbance peaks at 1321 and 920 cm^{-1} indicate the generation of the oxazine ring. The peak changes from 1508 to 1495 cm^{-1} can be attributed to the tetrasubstituted benzene ring. New peaks at 3141 cm^{-1} represents the incorporation of furan ring into Bz_TPf.

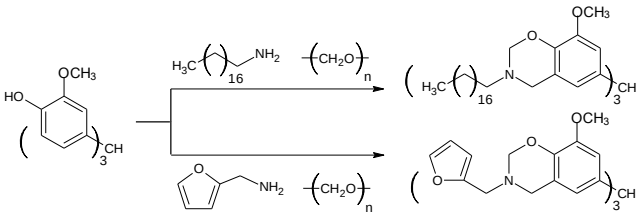

Scheme 2 Synthesis of Bz_TPo (upper) and Bz_TPf (lower).

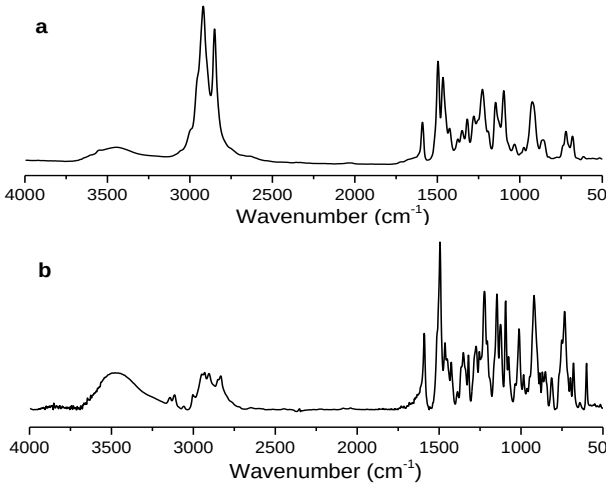

Fig. 2 FT-IR spectra of (a) Bz_TPo and (b) Bz_TPf**.**

All structures were further confirmed by the ^{1}H-NMR characterization (Figure 3). The trisubstituted benzene rings in TP give rise to the doublets at 6.81, 6.57 ppm and singlet at 6.62 ppm. The singlet at 5.34 ppm is due to the triphenyl methyl group. The integration value of the peak at 5.50 ppm is less than 3, which is attributed to the –OH active protons. The existence of $–OCH_3$ protons is evidenced by the singlet at 3.7[illegible] ppm. The characteristic oxazine rings in Bz_TPo are proved by the two resonances at 4.93 and 3.91 ppm, which represent the protons of N-CH_2-O and Ar-CH_2-N, respectively (Figure 3(b)). Another evidence is the tetrasubstituted benzene rings indicated by the peaks at 6.49 (singlet) and 6.24 ppm (singlet). The incorporation of octadecylamine in Bz_TPo is confirmed by the resonances at 2.74, 1.25 and 0.88 ppm. The triphenyl methyl structure gives the singlet at 5.21 ppm. Similar results can be found in the ^{1}H-NMR spectrum of Bz_TPf monomer (Figure 3(c)). Specifically, the generation of the oxazine rings are proved by the resonances at 4.96 and 3.95 ppm which represent the protons of N-CH_2-O and Ar-CH_2-N, respectively. The protons of furan rings give rise to the resonances at 7.40, 6.32 and 6.24 ppm, respectively.

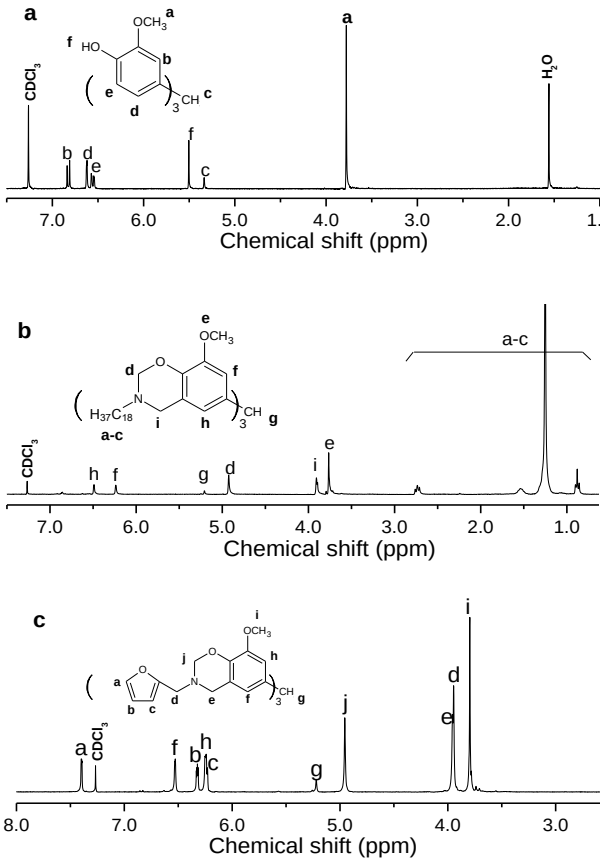

Fig. 3 ^{1}H-NMR spectra of (a) TP (b) Bz_TPo and (c) Bz_TPf.

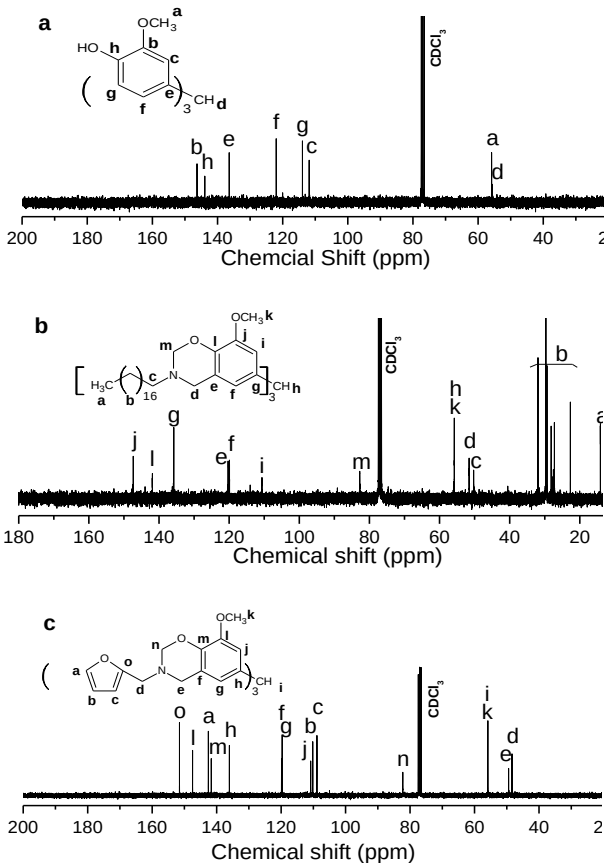

Fig. 4 ^{13}C-NMR spectra of (a) TP (b) Bz_TPo and (c) Bz_TPf.

Figure 4 shows the ^{13}C-NMR of TP, Bz_TPo and Bz_TPf. The resonance at 55.66 ppm indicates the trisubstituted methyl group and the peak at 136.41 ppm represents the adjacent carbons on the the benzene rings (Figure 4(a)). The ^{13}C-NMR spectra in Figure 4(b) and Figure 4(c) confirm the formation of the Bz_TPo and Bz_TPf. The characteristic oxazine rings are proved by the carbon resonances at 82.76 (O-CH_2-N), 51.57 (Ph-CH_2-N) ppm for Bz_TPo and 82.25 (O-CH_2-N), 49.43 (Ph-CH_2-N) ppm for Bz_TPf. The incorporation of long aliphatic chain in Bz_TPo can be proved by the peaks at 50.29 and 15-35 ppm. The existence of furan ring in Bz_TPf can be confirmed by the peaks at 142.57, 110.18 and 108.89 ppm. The peak appears at 48.38 corresponding to the –CH_2-N of the furan ring.

Moreover, MALDI-TOF was applied to further determine the molecular weight. The results have been summarized in the experimental session and in Figure S5, which are in good agreement with theoretical calculation. It is worth to note that the benzoxazine monomers can decompose during the measurement following the $[M+H-n*12]^{+}$ rule (Figure S5), which were reported by P. Vainiotalo et al and R. Quevedo et al before.[33,34] In sum, the above characterization results confirm the successful preparation of the molecules.

The polymerization behaviour of both TP based monomers were monitored by DSC. The results are summarized in Table 1. The endotherm peaks at 50°C and 165°C are the melting points of the monomers. The onset and maximum curing temperatures of Bz_TPo are around 216 and 240 °C, while lower temperatures at 209 and 234 °C can be found when cure Bz_TPf. The long alkyl chains can hinder the polymerization process and cause higher curing temperature of Bz_TPo than Bz_TPf. Meanwhile, the furan ring can participate into the polymerization while the alkyl chain is inert during the process.[35] The thermal stability of the monomers were examined through TGA (Figure 5), which show comparable results with most petroleum-based benzoxazine monomers reported by others. [36]

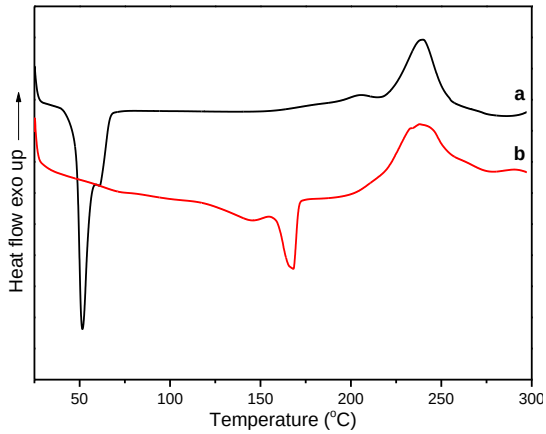

Fig. 5 DSC curves of (a) Bz_TPo and (b) Bz_TPf at heating rate of 10°C/min, respectively.

Table 1 DSC data of Bz_TPo and Bz_TPf monomers at a heating rate of 10K/min.

Monomer	T_m (°C)	T_{onset} (°C)	T_{max} (°C)	ΔH (J/g)
Bz_TPo	50	216	240	92
Bz_TPf	165	209	234	104

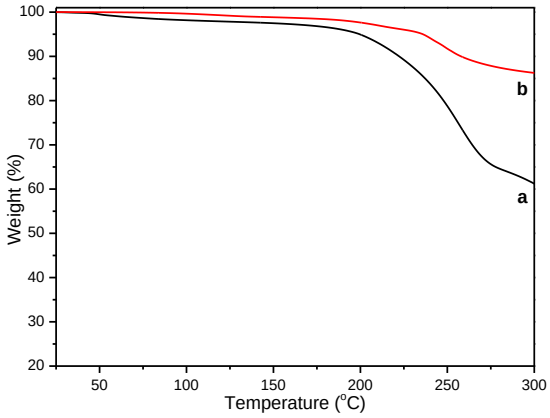

Fig. 6 TGA curves of monomers (a) Bz_TPo, (b) Bz_TPf.

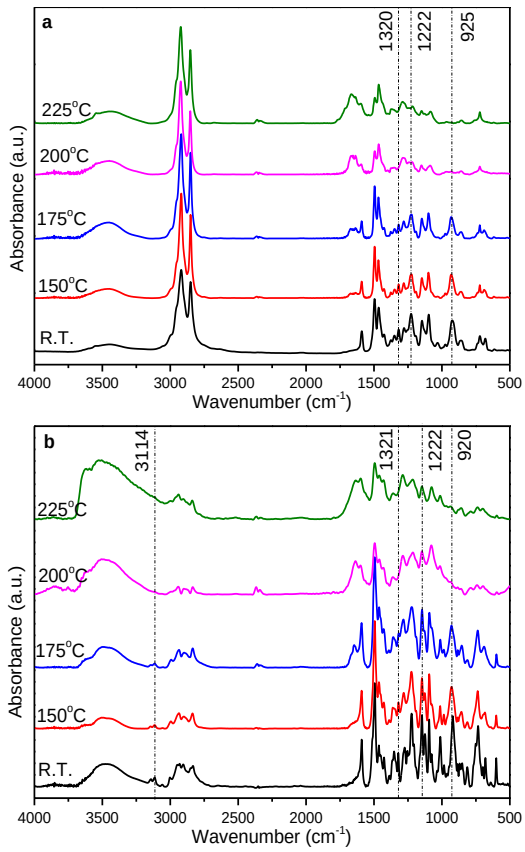

Fig. 7 FT-IR spectra of (a) Bz_TPo and (b) Bz_TPf cured at different temperatures for 1 hour.

Table 2 Solubility test of the polymers: PBz_TPo, PBz_TPf, PBz_Go and PBz_Gf, cured from the corresponding monomers.

Sample	Insoluble weight (%)
PBz_TPo	26.5
PBz_TPf	>99
PBz_Go	<5
PBz_Gf	10.8

In order to clarify the curing process, FT-IR was applied to monitor the changes in chemical structures. Figure 6 shows the FT-IR spectra of monomers cured at 150°C, 175°C, 200°C and 225°C in air for 1 hour, respectively. For both monomers, dramatic decrease in peak intensity around 920 (oxazine ring), 1222 (asymmetric stretching of C-O-C) and 1320 (CH_2 wagging of oxazine ring) indicates the oxazine ring-opening during polymerization.[37] Meanwhile, The peaks at 3100-3150 cm^{-1} (C-H, furan ring) and 1495 cm^{-1} (C-H, Ar) diminish at high temperature suggest the both furan ring and benzene ring involve the polymerization process.[38] As the process is similar to the Freidel-Crafts reaction, and the unchanged of peaks at 2920 and 2850 cm^{-1} (C-H, alkyl chain) proved the non-reactivity of the chain during polymerization. Therefore, only phenyl substitution stimulated by the positioning effect of methoxy group can take place when polymerize Bz_TPo,[16,18] while both benzene ring and furan ring are reactive when cure Bz_TPf. In order to study the influence of multi-oxazine rings to the polymer structure, solubility test of the cured polymers was implemented and the results were summarized in Table 2. For comparison, polymers prepared from Bz_Go and Bz_Gf (monomers with one oxazine-ring) were examined as well. Insoluble solids can be found among all the polymers, but the residue weight percentages are quite different. Comparing with polymers prepared from guaiacol, polybenzoxazines using TP as phenol source generate more insoluble residues after test. The results imply that multi-oxazine rings can significantly facilitate the formation of the cross-linked structures. The insoluble PBz_TPo indicates the substitution can take place on the benzene ring, as we mentioned before. Meanwhile, polymers show enhancement in cross-linking when furan ring was introduced, especially a fully insoluble PBz_TPf can be obtained by such kind of incorporation. Based on the experimental results and the iminium ion mechanism proposed by H. Ishida and J. Dunkers,[39] while later on extended by T. Endo, A. Sudo and their coworkers,[40] the related polymerization process for Bz_TPo and Bz_TPf are sketched in Scheme 3.

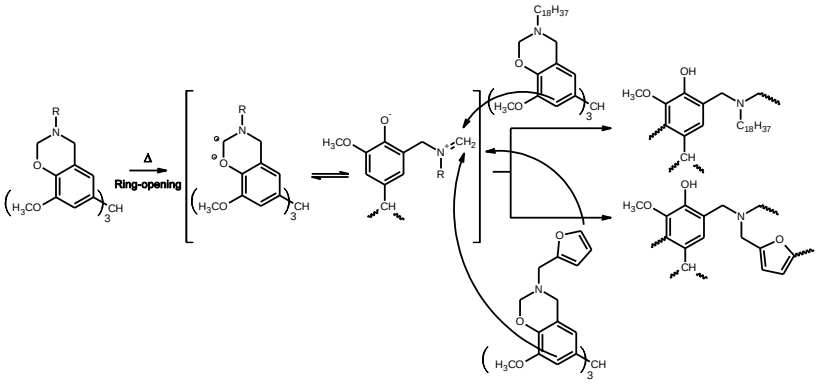

Scheme 3 Mechanism for the ring-opening polymerization of Bz_TPo and Bz_TPf.

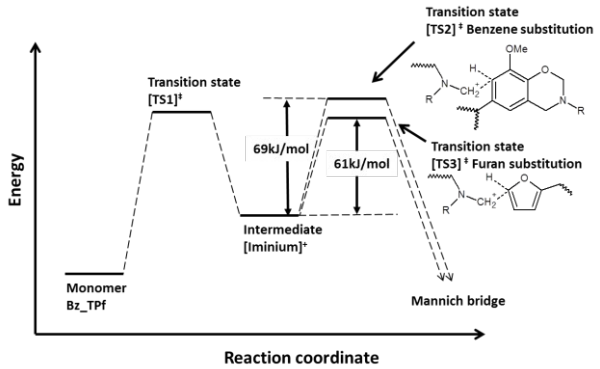

Scheme 4 Energy change during ring-opening polymerization of Bz_TPf.

In fact, although compete substitutions on furan and benzene rings had been observed by many other researchers as well,[16,18] the preference of the two pathways and the related kinetic analysis are still unknown so far. Moreover, the widely accepted ring-opening mechanism involved two main steps, which are the carbocation/ iminium generation and the electrophilic substitution.[41] Thus, many convenient methods, such as DSC, may not be suitable because the obtained activation energy value is only apparent.[42] For this reason, quantum chemistry calculation based on transition state theory was applied to estimate the energy changes during the two pathways. Since zwitter iminium intermediate generates within both pathways, only the energy differences between the intermediate and transition states of the electrophilic process need to be considered. The calculated energy results were showed in Scheme 4. The energy barrier between furan substituted transition state and iminium intermediate is 60.98kJ/mol, which is smaller than the benzene substituted structure (68.94kJ/mol), but not very significant. Therefore, based on the transition state theory understanding, substitution prefers to happen at the furan ring. However, it cannot determine the whole polymerization kinetics because many other factors may influence the reaction kinetics as well.[42] After all, the quantum chemistry calculation results provide useful information based on energy viewpoint for further analysing the sophisticated polymerization kinetics, to be exact.

The polymers were first characterized by DSC to determine their T_g (Figure 7). Generally, T_g is effected by both the rigidity of the polymer chain and the cross-linking density. As mentioned above, the PBz_TPf is more cross-linked than PBz_TPo, while the flexible long alkyl chain further lower the T_g of PBz_TPo. These reasons give rise to the T_g at 145°C of PBz_TPf and much lower T_g at 58°C of PBz_TPo. The mechanical performance of the PBz_TPf was checked through DMA (Figure 8). The T_g determined by loss modulus curve is 155°C, which is consistent with the result obtained from DSC.

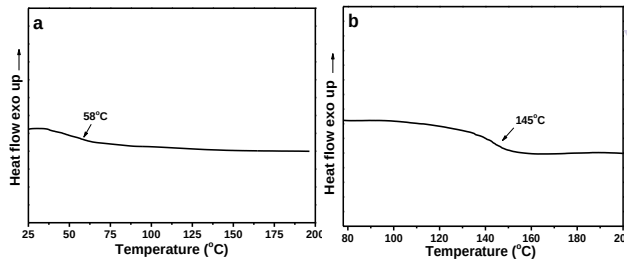

Fig. 8 DSC curves of (a) PBz_TPo and (b) PBz_TPf for T_g determination.

The thermal properties of PBz_TPo and PBz_TPf were examined through TGA (Figure 9). The results are concluded in Table 3. It is observed that PBz_TPf has higher degradation temperature than PBz_TPo. This can be understood through the enhancement in cross-linked structure by furan ring, thus eliminates the fragment decomposition.[38] Meanwhile, high char yield of PBz_TPf (60%) can be achieved at 800°C under nitrogen atmosphere due to the incorporation of the furan ring into the polymer. According to Van Krevelan and Hofytzer's equation, the value of char yield can be used to calculate the limiting oxygen index (LOI), which is used to evaluate the flame retardancy.[43] The LOI value of PBz_TPf is 41.3, which indicates the possible self-extinguishing performance. Meanwhile, it is worth to note that, the triphenyl methyl structure in the polybenzoxazines can be modified by reacting with phosphorus containing chemicals, such as DOPO, to further enhance their flame resistance.[44]

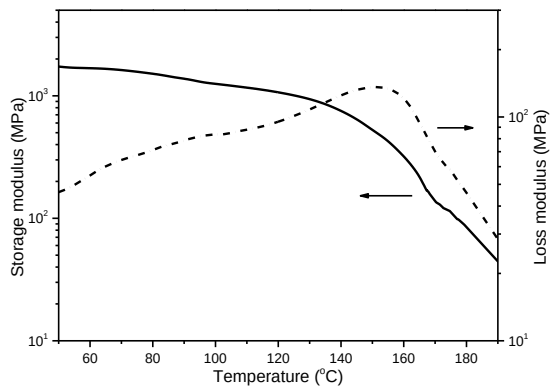

Fig. 9 Storage and loss modulus of PBz_TPf measured by DMA.

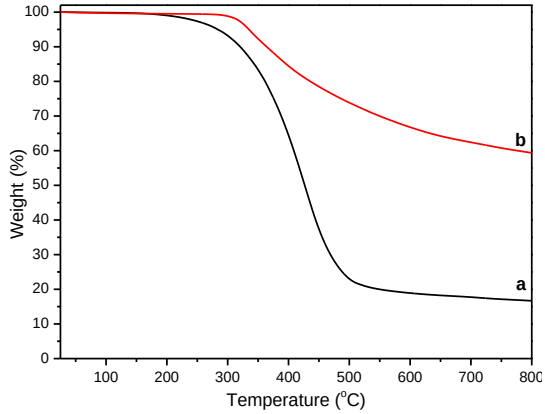

Fig. 10 TGA curves of (a) PBz_TPo and (b) PBz_TPf.

Table 3 TGA data of PBz_TPo and PBz_TPf Polymers.

Polymer	$T_d^{5\%}$ (°C)	$T_d^{10\%}$(°C)	Char yield (%)	LOI values
PBz_TPo	284	321	16.7	24.2
PBz_TPf	335	364	59.6	41.3

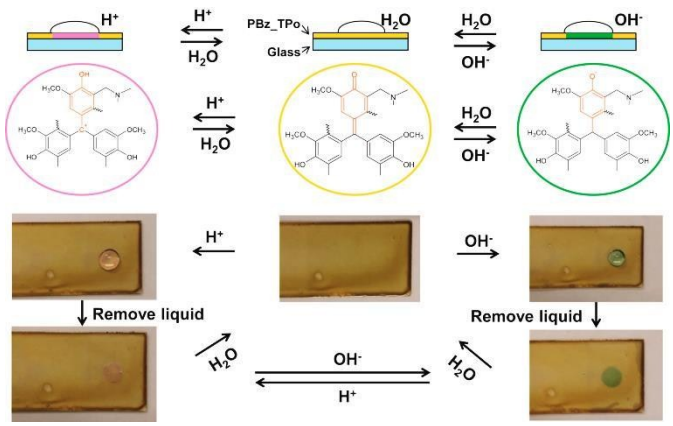

Fig. 11 Color change of PBz_TPo film on glass by adjusting the pH conditions.

Interestingly, by overviewing the experiment results, it was noticed that a carbonyl band gave rise to the high intensity at 1670 cm^{-1} after curing both of the monomers under high temperature (Figure 6). This is due to the oxidation of the phenol into a benzoquinone structure.[45] The process resulted in generating conjugated structures which are similar to some triphenyl dyes.[46] These dyes show vivid colors and some of them are pH-responsible. Therefore, it was suspected that the materials in this study may also have similar properties. The experiment was conducted by polymerizing a PBz-TPo film on glass. Acidic, neutral and basic liquids were dropped onto the glass, respectively, before color changes can be observed with several seconds (Figure 11). Moreover, the film can recover to its original color simply after washing by water. Such process was conducted at the same position for several times and reversible color changes can be observed.

Conclusions

Two fully renewable benzoxazine monomers with multi-oxazine rings were reported in this study. The structures of the TP and benzoxazine monomers were confirmed through FT-IR and NMR. The ring-opening polymerization was monitored through DSC analysis and confirmed through FT-IR spectra based on different curing temperatures. Related polymerization process was purposed. Furthermore, through comparing the solubility of different polymers, the multi-oxazine ring structure was proved to enhance the cross-linking. Moreover, enhancement in T_g, thermal stability and char yield can be found in the polybenzoxazines incorporated with furan rings. Besides, oxidation at high curing temperature resulted in a conjugated structure, which exhibits color change under different pH condition and can be easily recovered. In conclusion, the work shows the feasibility in preparing fully renewable polybenzoxazines based on monomers containing multi-oxazine rings. These polymers exhibit desirable properties as well as other smart functions.

Notes and references

1 H. Ishida, in: H. Ishida and T. Agag Ed., *Handbook of Benzoxazine Resins*, Amsterdam: Elsevier, **2011**, 3.
2 M. Comi, G. Lligadas, J. C. Ronda, M. Galia and V. Cadiz, *J. Polym. Sci., Part A: Polym. Chem.*, **2013**, 51, 4894.
3 K. Chiou and H. Ishida, Curr. *Organ. Chem.*, **2013**, 17, 913.
4 G. Lligadas, A. Tuzun, J. C. Ronda, M. Galia and V. Cadiz, *Polym. Chem.*, **2014**, 5, 6636.
5 A. Chernykh, T. Agag and H. Ishida, *Macromolecules*, **2009**, 42, 5121.
6 Y. Omura, Y. Taruno, Y. Irisa, M. Morimoto, H. Saimoto and Y. Shigemasa, *Tetrahedron Lett.*, **2001**, 42, 7273-7275.
7 A. Alwaige, T. Agag, H. Ishida and S. Qutubuddin, *RSC Adv.*, **2013**, 3, 16011-16020.
8 H. Kimura, Y. Murata, A. Matsumoto, K. Hasegawa, K. Ohtsuka and A. Fukuda, *J. Appl. Polym. Sci.*, **1999**, 74, 2266.
9 E. Calo, A. maffexxoli, G. mele, F. Maritina, S. E. mazzetto, Tarzia and C. Stifani, *Green Chem.*, **2007**, 9, 754.
10 C. Zhang, Y. Zhang, Q. Zhou, H. Ling and Y. Gu, *J. Polym. Eng.*, **2014**, 34, 561.
11 H. Xu, Z. Lu and G. Zhang, *RSC Adv.*, **2012**, 2, 2768.
12 P. Thirukumaran, A. Shakila and S. muthusamy, *RSC Adv.*, **2014**, 4, 7959.
13 H. Oie, A. Sudo, T. Endo, *J. Polym. Sci., Part A: Polym. Chem.*, **2013**, 51, 2035.

14 L. Dumas, L. Bonnaud, M. Olivier, M. Poorteman and P. Dubois, *J. Mater. Chem. A*, **2015**, 3, 6012.
15 M. Kleinert and T. Barth, *Chem. Eng. Technol.*, **2008**, 31, 736.
16 C. F. Wang, J. Q. Sun, X. D. Liu, A. Sudo and T. Endo, *Green Chem.*, **2012**, 14, 2799.
17 http://www.borregaard.com.
18 A. Van, K. Chiou and H. Ishida, *Polymer*, **2014**, 55, 1443.
19 N. K. Sini, J. Bijwe and I. K. Varma, *J. Polym. Sci., Part A: Polym. Chem.*, **2014**, 52, 7.
20 G. Riess, L. J. Schwob, G. Guth, M. Roche and B. Lande, in: B. M. Culbertson and J. E. Mcgrath Ed., *Advances in Polymer Science*, New York: Plenum, **1986**, 27.
21 A. Laobuthee, S. Chirachanchai, H. Ishida and K. Tashiro, *J. Am. Chem. Soc.*, **2001**, 123, 9947.
22 S. Chirachanchai, A. Laobuthee and S. Phongtamrug, *J. Heterocyclic Chem.*, **2009**, 46, 714.
23 Z. Brunovska and H. Ishida, *J. Appl. Polym. Sci.*, **1999**, 73, 2937.
24 X. Ning, H. Ishida, *J. Polym. Sci. Chem. Ed.*, **1994**, 32, 1121.
25 T. Takeichi, T. Kano and T. Agag, *Polymer*, **2005**, 46, 12172.
26 K. D. Demir, B. Kiskan, B. Aydogan and Y. Yagci, *React. Func. Polym.*, **2013**, 73, 346.
27 T. Agag and T. Takeichi, *J. Polym. Sci., Part A: Polym. Chem.*, **2007**, 45, 1878.
28 C. Zuniga, G. Lligadas, J. C. Ronda, M. Galia and V. Cadiz, *Polymer*, **2012**, 53, 1617.
29 S. Li and S. Yan, *RSC Adv.*, **2015**, 5, 61808.
30 N. K. Sini, J. Bijwe and I. K. Varma, *Polym. Degrad. Stabil.*, **2014**, 109, 270.
31 T. Agag, S. Geiger and H. Ishida, in: H. Ishida and T. Agag Ed., *Handbook of Benzoxazine Resins*, Amsterdam: Elsevier, **2011**, 263.
32 Gaussian 09, Revision D.1, M. J. Frisch, G. W. Trucks, H. B. Schlegel, G. E. Scuseria, M. A. Robb, J. R. Cheeseman, G. Scalmani, V. Barone, B. Mennucci, G. A. Petersson, H. Nakatsuji, M. Caricato, X. Li, H. P. Hratchian, A. F. Izmaylov, J. Bloino, G. Zheng, J. L. Sonnenberg, M. Hada, M. Ehara, K. Toyota, R. Fukuda, J. Hasegawa, M. Ishida, T. Nakajima, Y. Honda, O. Kitao, H. Nakai, T. Vreven, J. A. Montgomery, Jr., J. E. Peralta, F. Ogliaro, M. Bearpark, J. J. Heyd, E. Brothers, K. N. Kudin, V. N. Staroverov, R. Kobayashi, J. Normand, K. Raghavachari, A. Rendell, J. C. Burant, S. S. Iyengar, J. Tomasi, M. Cossi, N. Rega, J. M. Millam, M. Klene, J. E. Knox, J. B. Cross, V. Bakken, C. Adamo, J. Jaramillo, R. Gomperts, R. E. Stratmann, O. Yazyev, A. J. Austin, R. Cammi, C. Pomelli, J. W. Ochterski, R. L. Martin, K. Morokuma, V. G. Zakrzewski, G. A. Voth, P. Salvador, J. J. Dannenberg, S. Dapprich, A. D. Daniels, Ö. Farkas, J. B. Foresman, J. V. Ortiz, J. Cioslowski, and D. J. Fox, Gaussian, Inc., Wallingford CT, **2009**.
33 K. Hakala, J. M. J. Nuutinen, T. Straub, K. Rissanen and P. Vainiotalo, *Rapid Commun. Mass Spectrom.*, **2002**, 16, 1680-1685.
34 N. Nunez-Dallos, A. Reyes and R. Quevedo, *Tetrahedron Lett.*, **2012**, 53, 530-534.
35 Y. L. Liu and C. I. Chou, *J. Polym. Sci., Part A: Polym. Chem.*, **2005**, 43, 5267.
36 X. Ning, H. Ishida, *J. Polym. Sci. Phys.*, **1994**, 32, 921.
37 X. Q. Zhang, M. G. Looney, D. H. Solomon and A. K. Whittaker, *Polymer*, **1997**, 38, 5835.
38 P. Thirukumaran, P. A. Parveen, K. Kumudha and M. Sarojadevi, *Polym. Compos.*, **2014**, 10.1002/pc.23356.
39 J. Dunkers and H. Ishida, *J. Polym. Sci. Part. A. Polym. Chem.*, **1999**, 37, 1913–1921.
40 A. Sudo, R. Kudoh, H. Nakayama, K. Arima and T. Endo, *Macromolecules*, **2008**, 41, 9030–9034.
41 H. D. Kim, H. Ishida, *Macromolecules*, **2000**, 33, 2839-2847.
42 A. Rucigaj, B. Alic, M. Krajnc and U. Sebenik, *Express Polym. Lett.*, **2015**, 9, 647.
43 M .Sponton, G. Lligadas, J. C. Ronda, M. Galia and V. Cadiz, *Polym. Degrad. Stabil.*, **2009**, 94, 1693.
44 C. H. Lin, S. X. Cai, T. S. Leu, T. Y. Hwang and H. H. Lee, *J. Polym. Sci., Part A: Polym Chem.*, **2006**, 44, 3454.
45 D. J. Allen and H. Ishida, *Polymer*, **2007**, 48, 6763.
46 P. Ollikka, K. Alhonmaki, V. M. Leppanen, T. Glumoff, T. Raijola and I. Suominen, *Appl. Environ. Microbiol.*, **1993**, 59, 4010.

Fully renewable Polybenzoxazines prepared from monomers with multi-oxazine rings shows reversible pH responsiveness, good thermal and mechanical performance.